



STRUCTURAL SCIENCE
CRYSTAL ENGINEERING
MATERIALS

Volume 76 (2020)

Supporting information for article:

Crystal structures of two very similar $2\times2\times2$ superstructures of γ -brass related phases in ternary Ir-Cd-Cu system

Sivaprasad Ghanta, Nilanjan Roy and Partha Pratim Jana

Table S1 Loaded reaction compositions and refined compositions obtained by single crystal X-ray diffraction in the Ir-Cd-Cu system.

Samp le code	Nominal Compositi on	Refined Composition (atomic %)	EDS Composition (atomic %)	VEC	Mai n phas e	Ir ₈ Cd ₄	Element al Cd	CuO (I4/mm m)
S1	Ir ₈ Cd ₄₁	Ir _{16.33} Cd _{83.67}	Ir _{16.09(1)} Cd _{83.91(1)}	1.96	+			
S2	Ir ₈ Cd ₃₈ Cu ₃	Ir _{7.252} Cd _{85.666} Cu _{7.1} 02	Ir _{9.18(0)} Cd _{83.08(0)} Cu _{7.75(} 0)	1.91	+	+		
S3	Ir ₈ Cd ₃₇ Cu ₄	Ir _{6.655} Cd _{85.809} Cu _{7.5} 35	Ir _{7.97(1)} Cd _{83.04(1)} Cu _{8.98(} 1)	1.92	+	+		
S6	Ir ₈ Cd ₃₆ Cu ₅	Ir _{5.474} Cd _{77.809} Cu _{16.} 716	Ir _{6.85(0)} Cd _{77.08(1)} Cu _{16.0} 6(1)	1.83	+	+	+	
S4	Ir ₈ Cd ₃₃ Cu ₈	Ir _{5.717} Cd _{79.040} Cu _{15.} 243	Ir _{6.35(1)} Cd _{77.93(1)} Cu _{15.7} 2(1)	1.85	+	+	+	
S5	Ir ₈ Cd ₂₉ Cu ₁₂	Ir _{5.164} Cd _{79.461} Cu _{15.} 374	Ir _{6.48(1)} Cd _{77.17(1)} Cu _{16.3} 5(1)	1.85	+	+		
S7	Ir ₈ Cd ₄₀ Cu ₁	-	Ir _{16.60(1)} Cd _{82.19(1)} Cu _{1.2} 1(1)		+			
S8	Ir ₈ Cd ₃₉ Cu ₂	-	Ir _{15.95(1)} Cd _{82.29(1)} Cu _{1.7} 6(1)		+			+

*Two unidentified extra peaks were observed for S8 at $2\theta = 34.9$, and 44.9 deg.

e/a for Ir, Cu and Cd was adopted from Mizutani *et al.* ($Ir = 1.60 VEC$, $Cu = 1 VEC$, and $Cd = 2.03 VEC$).
(Mizutani & Sato, 2017)

Table S2 Loaded reaction compositions and refined lattice parameters obtained by powder XRD data.

Sample code	Nominal Composition	lattice parameters (Å)		Space Group
S1	Ir ₈ Cd ₄₁	14.8582(9)	15.9929(10)	<i>R</i> $\bar{3}$
S2	Ir ₈ Cd ₃₈ Cu ₃	19.9487(10)		<i>F</i> $\bar{4}3m$
S3	Ir ₈ Cd ₃₇ Cu ₄	19.961(7)		<i>F</i> $\bar{4}3m$
S6	Ir ₈ Cd ₃₆ Cu ₅	19.7296(19)		<i>F</i> $\bar{4}3m$
S4	Ir ₈ Cd ₃₃ Cu ₈	19.741(3)		<i>F</i> $\bar{4}3m$
S5	Ir ₈ Cd ₂₉ Cu ₁₂	19.639(2)		<i>F</i> $\bar{4}3m$
S7	Ir ₈ Cd ₄₀ Cu ₁	14.8402(3)	15.9931(4)	<i>R</i> $\bar{3}$
S8	Ir ₈ Cd ₃₉ Cu ₂	14.8383(4)	15.9860(5)	<i>R</i> $\bar{3}$

Table S3 $2\times 2\times 2$ superstructure of γ -brass related phases with isolated cluster units (Cubic space group: *F* $\bar{4}3m$).

Compound	<i>cF...</i>	Cluster types*				
(Fe,Ni)Zn _{6.5}	408	γ	bcc/ γ		α -Mn/ γ (-CC)	Ti ₂ Ni
(Lidin <i>et al.</i> , 1994)		Zn ₂₆	(Fe, Ni) _{10.68} ^{CC,OT,OH} Zn ₁₆	Zn ₂₉	(Fe, Ni) ₄ ^{OT} Zn ₁₈	
Ir _{7+7δ} Zn _{97-11δ}	406-	γ	bcc/ γ		α -Mn/ γ	Ti ₂ Ni
(Hornfeck <i>et al.</i> , 2004)	403	Ir ₄ ^{OT} Zn ₂₂	Ir _{1-δ+m} ^{CC,OT,OH} Zn _{26-m}	Zn _{29-3δ}	Ir ₄ ^{OT} Zn ₁₈	
Ir _{6.698} Cd _{86.366}	403-	γ	bcc		Ti ₂ Ni	γ
Cu _{7.584} (S3)	404	(Cu, Cd) ₈ ^{IT,OT} Cd ₁₈ ^{OH,CO}	Cu ₁ ^{CC} (Cu, Cd) ₄ Cd ₄ ^{CB} (Cu, Cd) ₆ ^{OH} Cd	Ir ₄ ^{OT} Cd ₁₈ ^{OH,CO}	(Cu, Cd) ₄ ^{IT} (Ir, Cd) ₄ ^{OT} Cd ₁₈ ^{OH,CO}	
Ir _{5.873} Cd _{81.199}	411	γ	α -Mn		Ti ₂ Ni	γ
Cu _{15.659} (S4)		Cu ₁₀ ^{IT,OH} (Cu, Cd) ₄ ^{OT} Cd ₁₂ ^{CC}	Cu ₁ ^{CC} (Cu, Cd) ₄ ^{OT} Cd ₂₄ ^{TT,CO}	(Cu, Cd) ₆ ^{OH} Ir ₄ ^{OT} Cd ₁₂ ^{CC}	Cd ₂₂ ^{IT,OH,CO} (Ir, Cd) ₄ ^{OT}	

*Cluster types are presented around the high symmetric points of the unit cell.

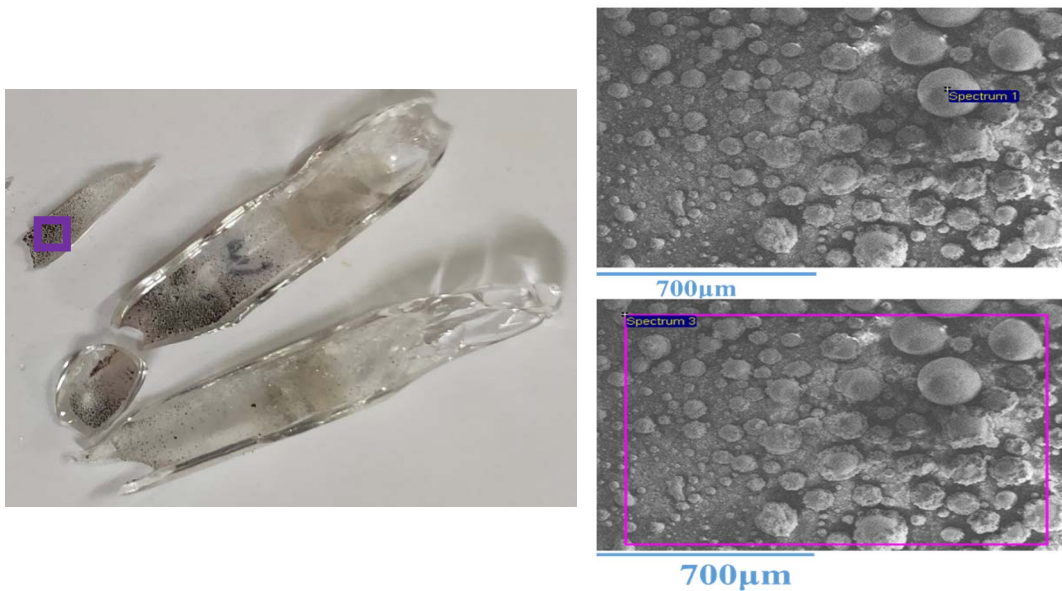


Figure S1 Image of the broken quartz tubes after heat treatment. Some amount of elemental cadmium vaporized and condensed on the inner wall of quartz tubes confirmed by SEM-EDS analysis.

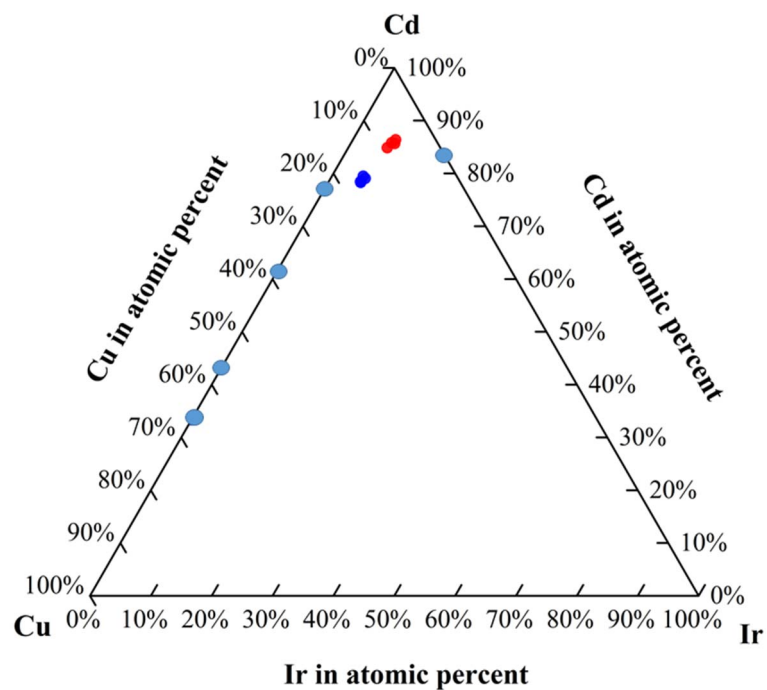


Figure S2 Measured compositions of Ir-Cu-Cd alloys with two closely γ -brass related phases are having the same space group ($F\bar{4}3m$). Additionally, the binary phases are represented with sky blue color (in the CuCd & IrCd system).

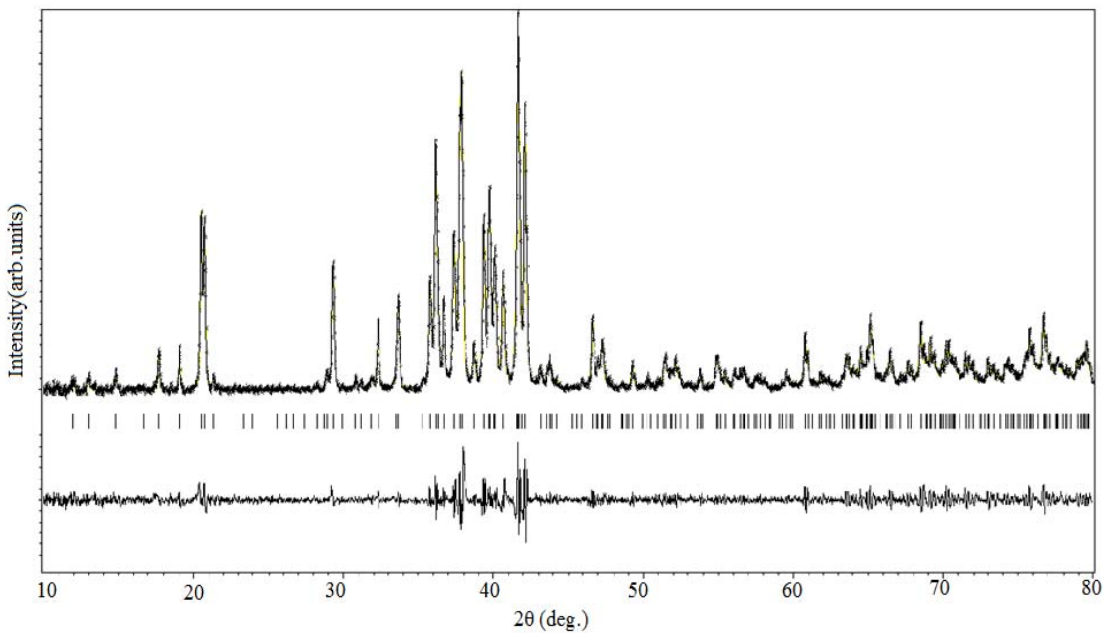


Figure S3 Profile fit for the loaded composition Ir₈Cd₄₁ (S1) (using Jana2006).

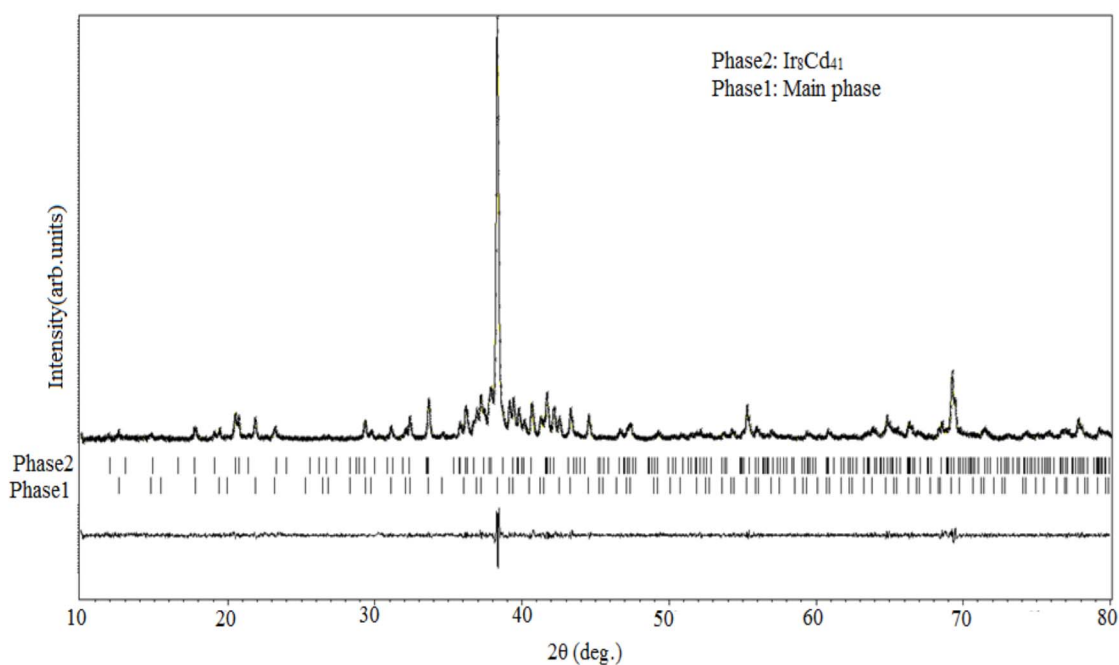


Figure S4 Profile fit for the loaded composition $\text{Ir}_8\text{Cd}_{38}\text{Cu}_3$ (S2).

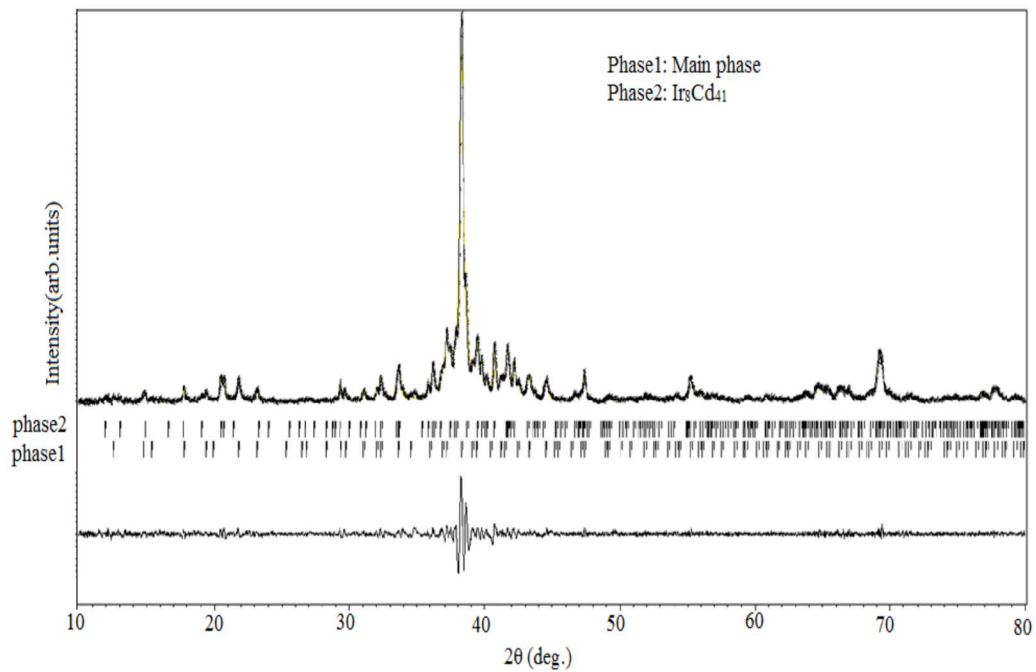


Figure S5 Profile fit for the loaded composition $\text{Ir}_8\text{Cd}_{37}\text{Cu}_4$ (S3).

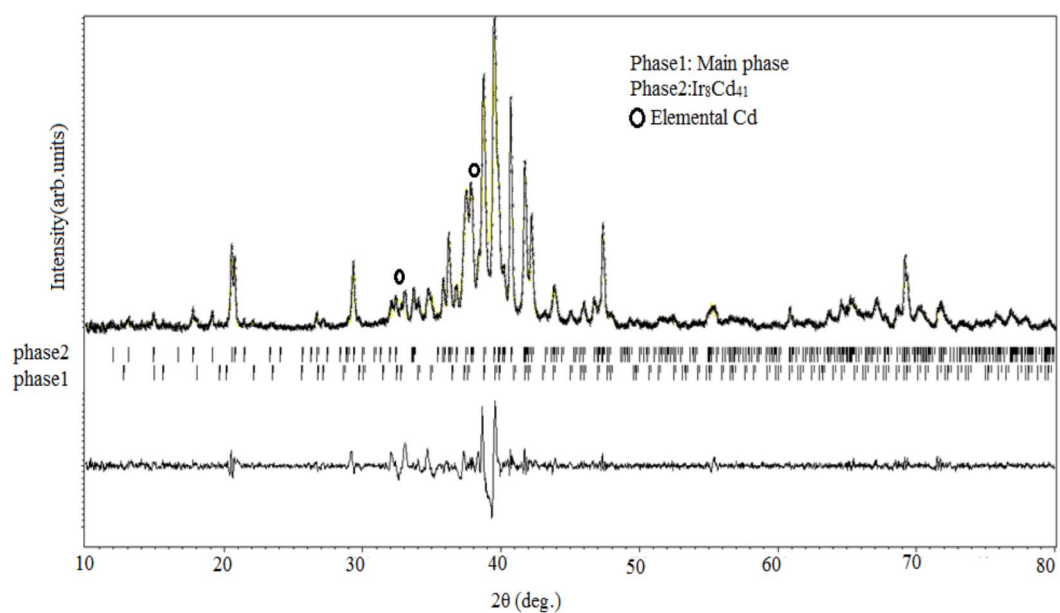


Figure S6 Profile fit for the loaded composition $\text{Ir}_8\text{Cd}_{36}\text{Cu}_5$ (S6).

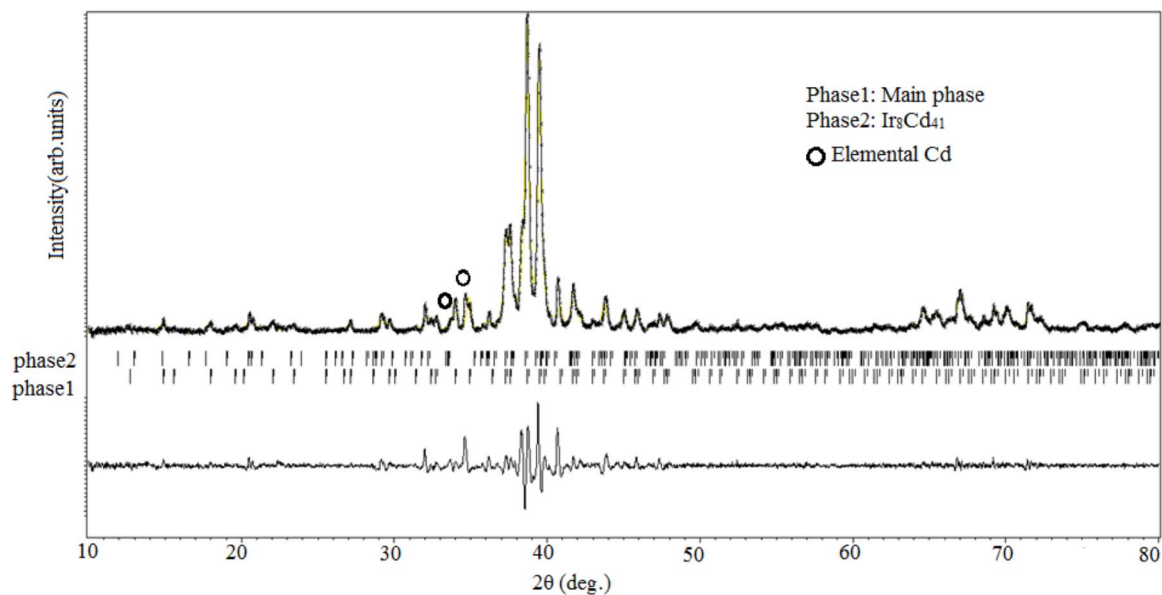


Figure S7 Profile fit for the loaded composition $\text{Ir}_8\text{Cd}_{33}\text{Cu}_8$ (S4).

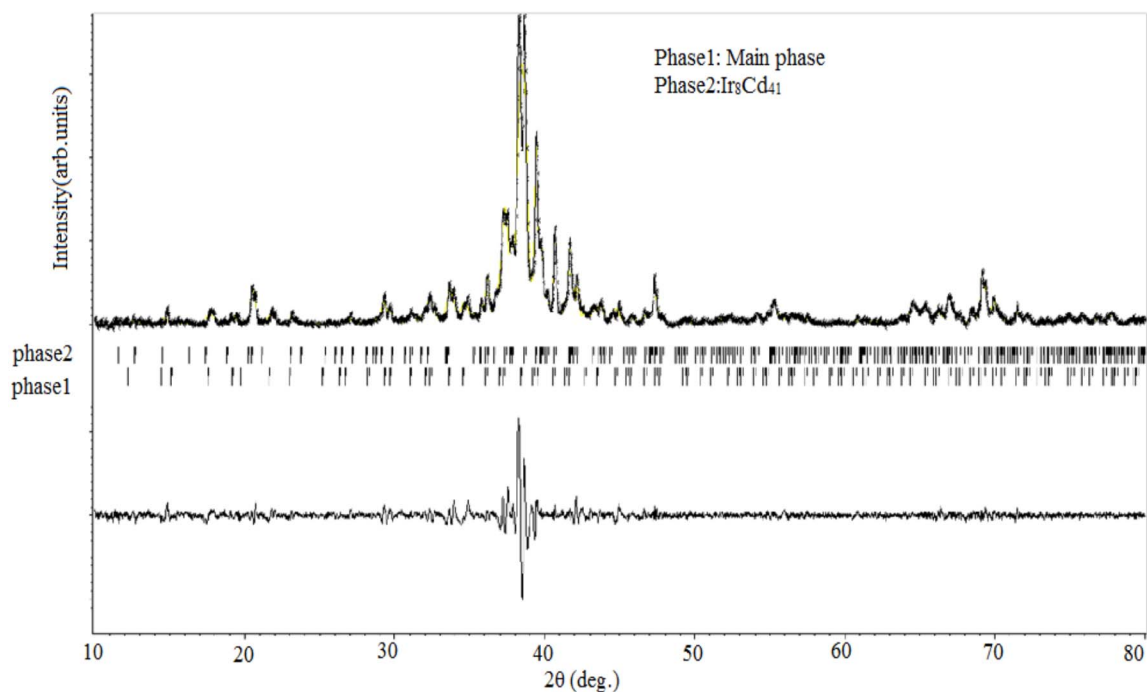


Figure S8 Profile fit for the loaded composition $\text{Ir}_8\text{Cd}_{29}\text{Cu}_{12}$ (S5).

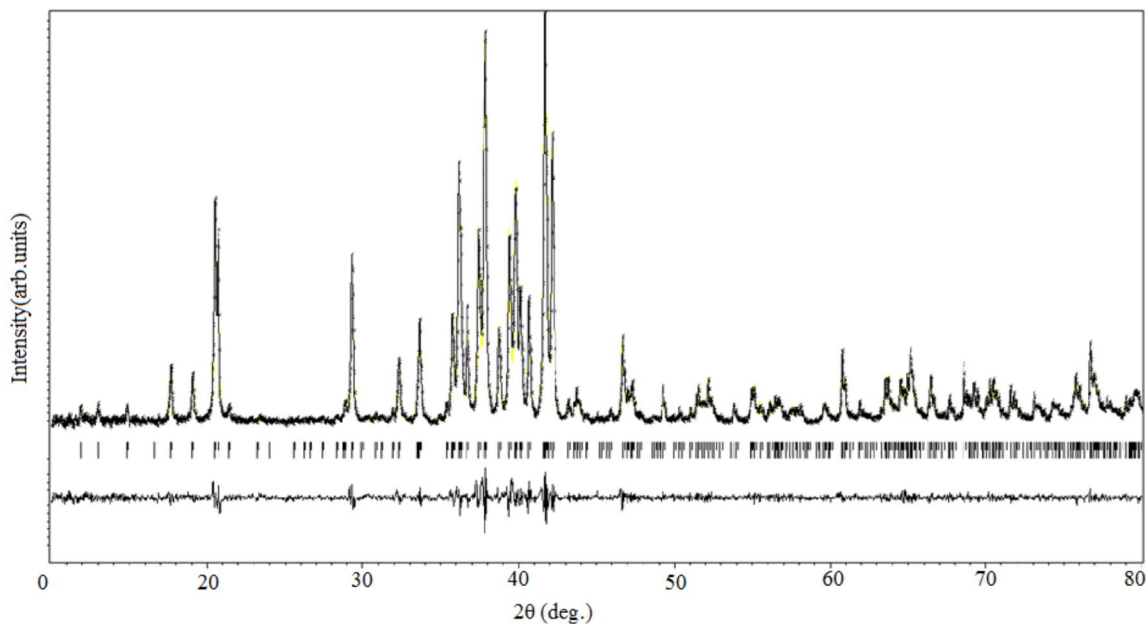


Figure S9 Profile fit for the loaded composition $\text{Ir}_8\text{Cd}_{40}\text{Cu}_1$ (S7).

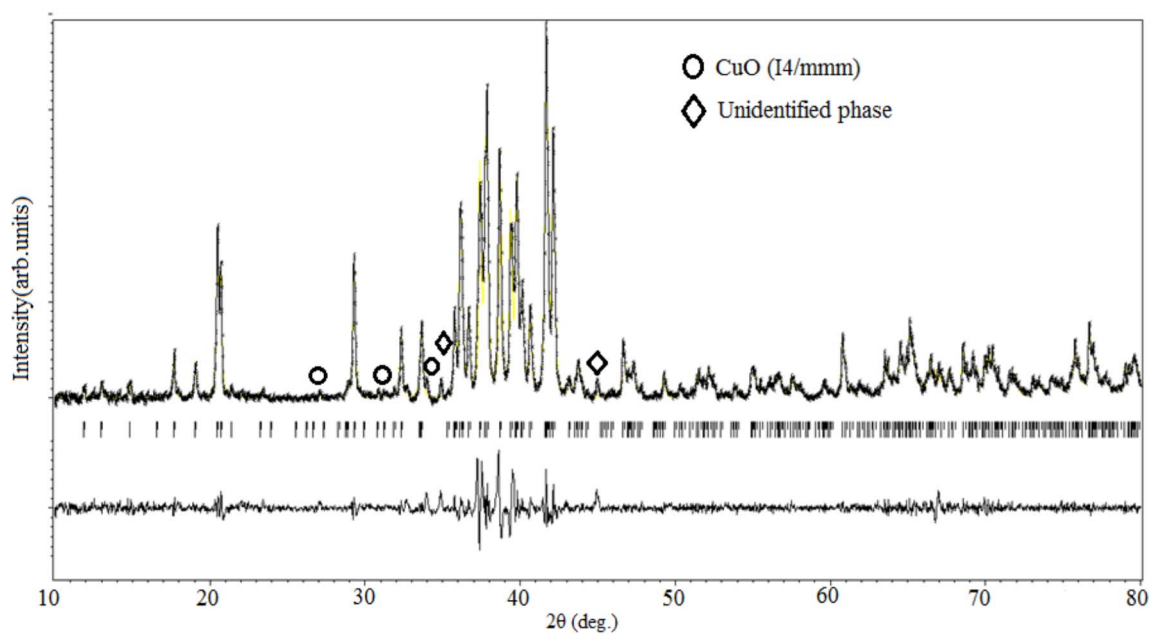


Figure S10 Profile fit for the loaded composition $\text{Ir}_8\text{Cd}_{39}\text{Cu}_2$ (S8).

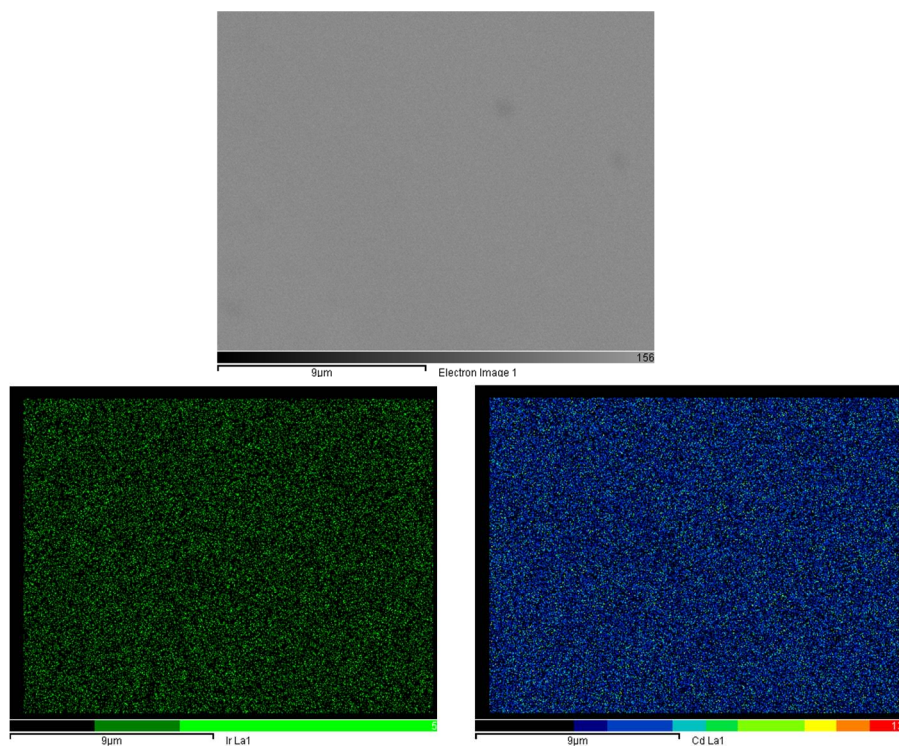


Figure S11 SEM Image with EDS distribution maps of loaded composition $\text{Ir}_8\text{Cd}_{41}$ (S1) (Colour Code for all samples: Green colour, Ir ; Blue colour, Cd; Brown colour, Cu) (Scale: 9μm).

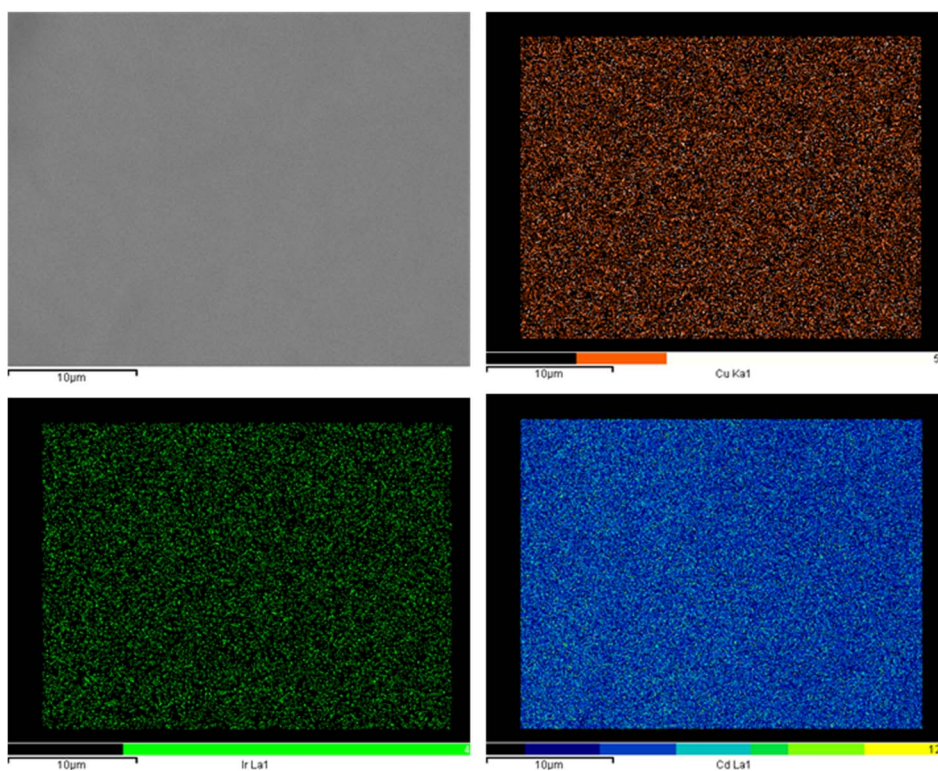


Figure S12 SEM Image with EDS distribution maps of loaded composition Ir₈Cd₃₈Cu₃ (S2) (Scale: 10 μm).

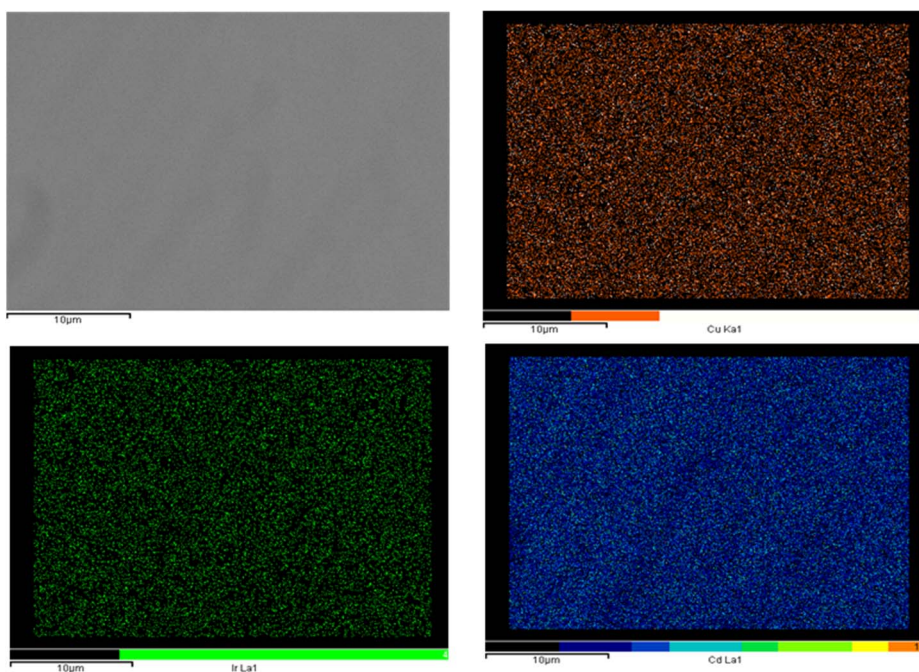


Figure S13 SEM Image with EDS distribution maps of loaded composition Ir₈Cd₃₈Cu₄ (S3) (Scale: 10 μm).

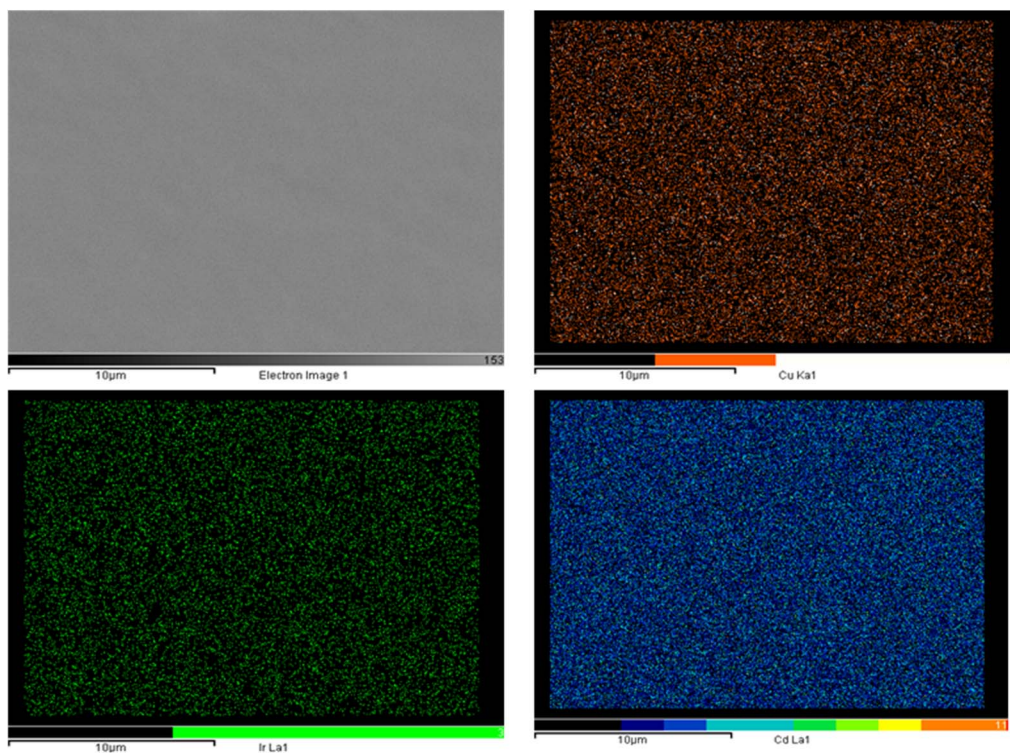


Figure S14 SEM Image with EDS distribution maps of loaded composition $\text{Ir}_8\text{Cd}_{38}\text{Cu}_5$ (S6) (Scale: 10 μm).

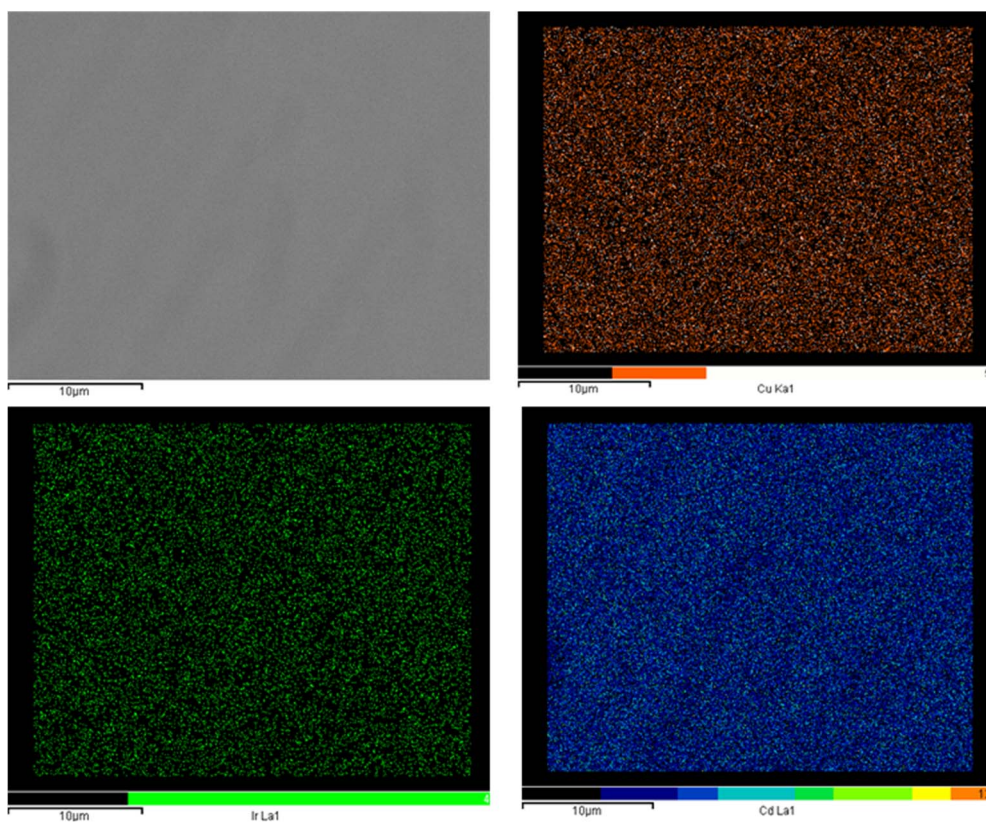


Figure S15 SEM Image with EDS distribution maps of loaded composition $\text{Ir}_8\text{Cd}_{33}\text{Cu}_8$ (S4) (Scale: 10 μm).

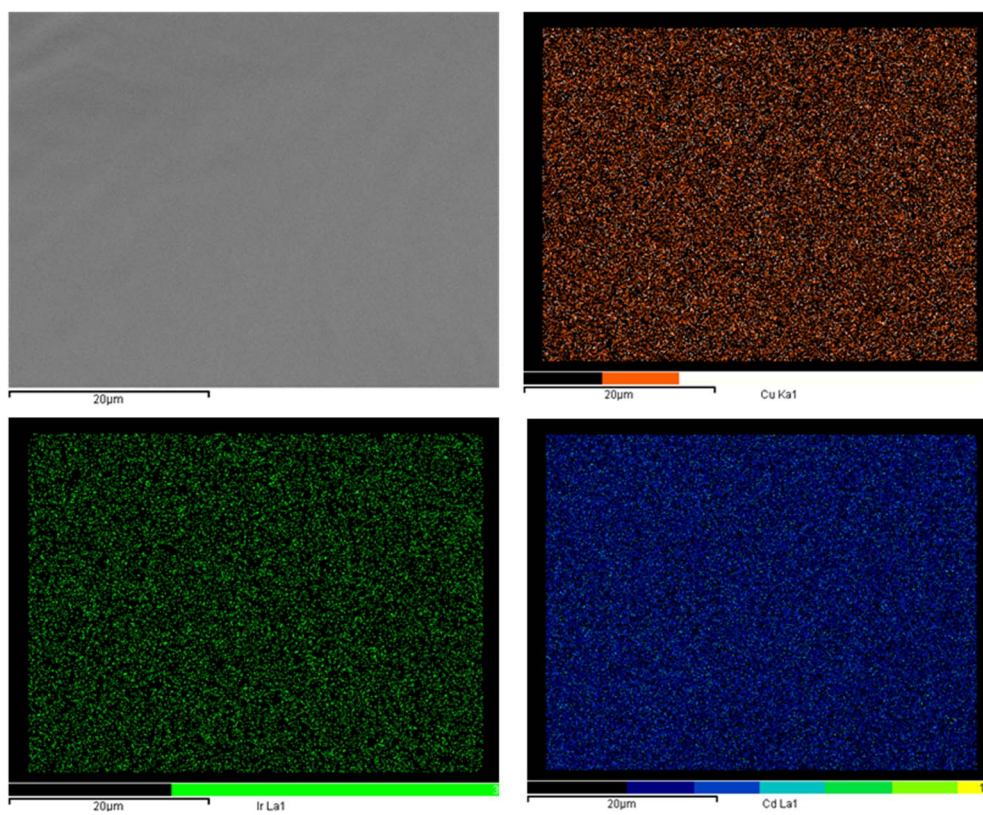


Figure S16 SEM Image with EDS distribution maps of loaded composition Ir₈Cd₂₉Cu₁₂ (S5) (Scale: 20 µm).

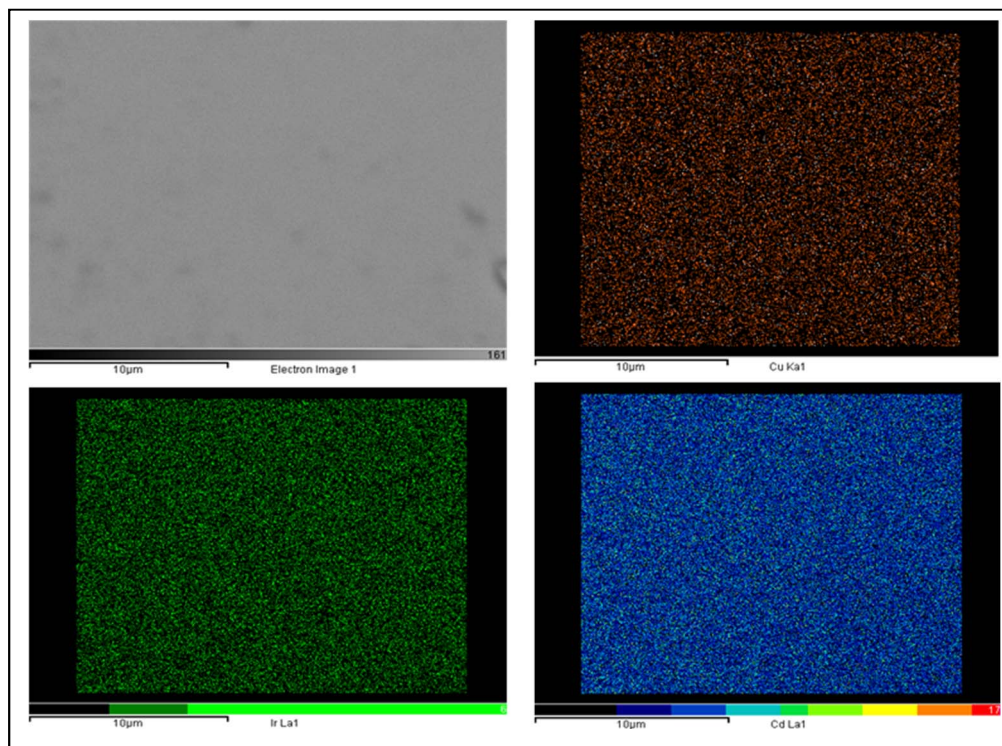


Figure S17 SEM Image with EDS distribution maps of loaded composition Ir₈Cd₄₀Cu₁ (S7) (Scale: 10 µm).

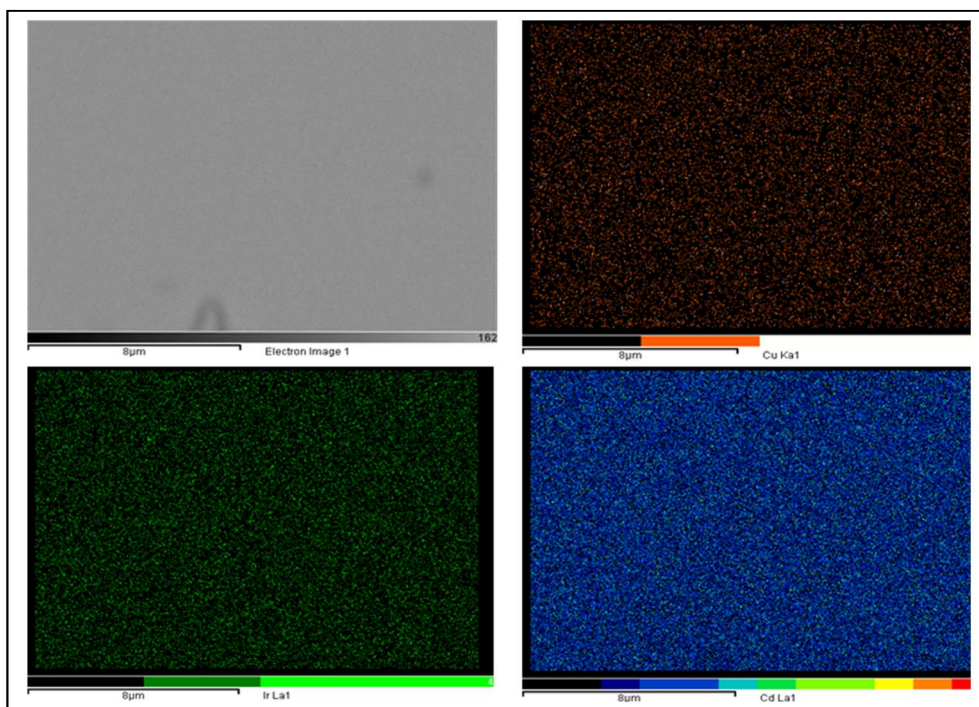


Figure S18 SEM Image with EDS distribution maps of loaded composition $\text{Ir}_8\text{Cd}_{39}\text{Cu}_2$ (S8) (Scale: 8 μm).